Supplementary Information

New homochiral ferroelectric supramolecular networks of complexes constructed by chiral *S*-naproxen ligand

Yong-Tao Wang,*[a] Gui-Mei Tang,[a] Wen-Zhu Wan,[a] Yue Wu,[a] Ting-Cui Tian,[a] Jin-Hua Wang,[a] Chao He,[b] Xi-Fa Long,*[b] Jun-Jie Wang,[c] and Seik Weng Ng*[d]

[a] Department of Chemical Engineering, Shandong Provincial Key Laboratory of Fine Chemicals, Shandong Polytechnic University, Jinan, 250353, P. R. China.

[b] Fujian Institute of Research on the Structure of Matter, Chinese Academy of Science, Fuzhou, 350002, P. R. China.

[c] Department of Chemistry, Anyang Normal University, Henan, 455002, P. R. China.

[d] Department of Chemistry, University of Malaya, Kuala Lumpur, 50603, Malaysia

* Corresponding author. E-mail: ceswyt@sohu.com. Fax: +086 0531 8900 0551; 8900 0551. E-mail: lxf@fjirsm.ac.cn. Fax: Int. code +86 0591 8371 4946. E-mail: seikweng@um.edu.my. Fax: (+60) 603 7967 4193.

Thermogravimetric analysis (TGA)

In order to estimate the stability of complexes, their thermal behaviours were studied by TGA technique. The experiments were performed on samples composed of numerous single crystals of **1**-**5** under N_2 atmosphere with a heating rate of 10 $^oC \cdot min^{-1}$ in the range of 30 to 700 ^oC (Fig. S18, see ESI). The TGA curve of complex **1** showed that the weight loss of 19.11% between 40 and 160 °C occurs, which can be ascribed to the loss of lattice and coordination water molecules (calculated: 21.77%). Decomposition of **1** began at about 288 ^oC, thus forming an unidentified product. For complex **2**, the first weight loss from 30 to 150 °C corresponds to the departure of lattice and coordinated water molecules (experimental: 13.72%, calculated: 12.12%). The decomposition of naproxen ligands occurs in the temperature range 210−358 °C (experimental: 78.25%, calculated: 77.09%). Upon further increasing the temperature, resulting into the formation of an unidentified product as the residue. For **3**, a weight loss of 7.15% is observed between 30 and 180 °C, which can be assigned to the release of the free and coordination water molecules per formula unit (calculated: 8.32%). The anhydrous compound started decompounding at about 260 °C. The residue was ZnO. For complex **4**, the weight loss occurs in the temperature range 30-180 ^oC in the TGA curve, which can be attributed to the loss of free and coordinated water molecules (experimental: 6.03%, calculated: 8.64%). Above 310°C, rapid weight loss occurred owing to the decomposition of the organic ligands. Complex **5** releases its coordinated water molecules gradually from 90 to 180 °C (obsd 3.26%, calcd 3.06%). The decomposition of the organic components occurs at 300 °C. The resdiue was CdO (experimental: 18.83%, calculated: 21.80%).

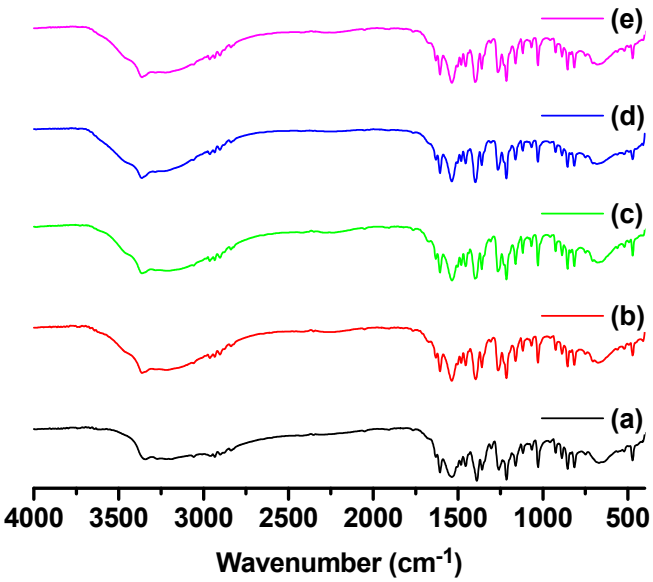

Fig. S1 IR spectra for **1** prepared by a series of nickel salts with different anions respectively: (a) SO_4^{2-}; (b) NO_3^-; (c) ClO_4^-; (d) Cl^- ; (e) Ac^-.

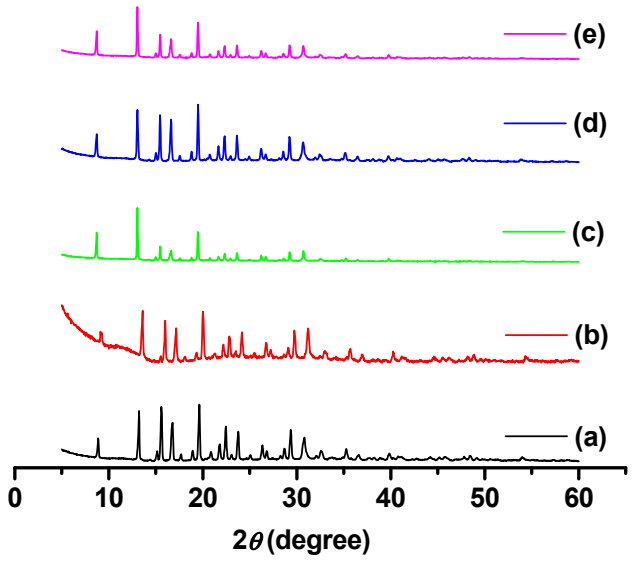

Fig. S2 Powdered X-Ray diffraction (PXRD) patterns for **1** obtained by a series of nickel salts with different anions respectively: (a) SO_4^{2-}; (b) NO_3^-; (c) ClO_4^-; (d) Cl^-; (e) Ac^-.

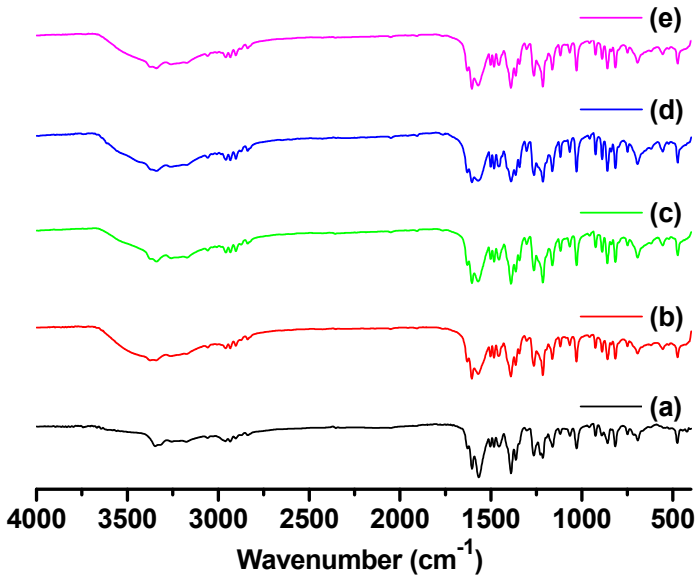

Fig. S3 IR spectra for **2** prepared by a series of copper salts with different anions respectively: (a) SO_4^{2-}; (b) NO_3^-; (c) ClO_4^-; (d) Cl^-; (e) Ac^-.

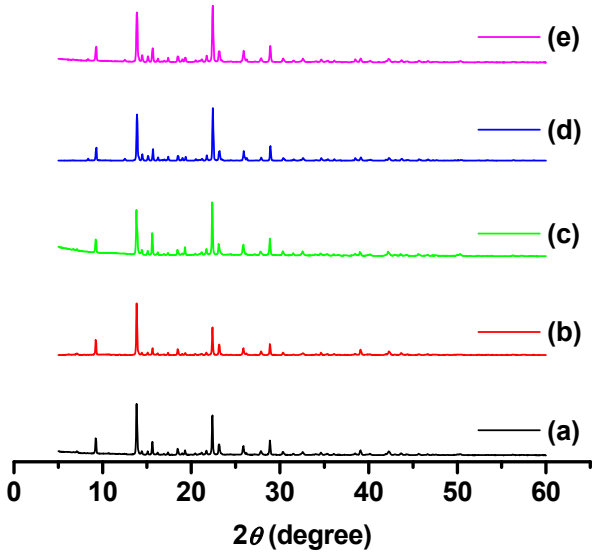

Fig. S4 PXRD patterns for **2** obtained by a series of copper salts with different anions respectively: (a) SO_4^{2-}; (b) NO_3^-; (c) ClO_4^-; (d) Cl^-; (e) Ac^-.

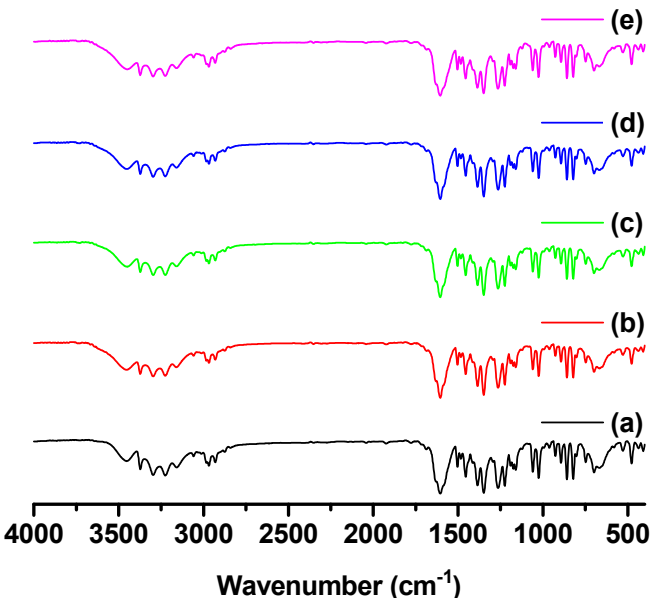

Fig. S5 IR spectra for **3** prepared by a series of zinc salts with different anions respectively: (a) SO_4^{2-}; (b) NO_3^-; (c) ClO_4^-; (d) Cl^-; (e) Ac^-.

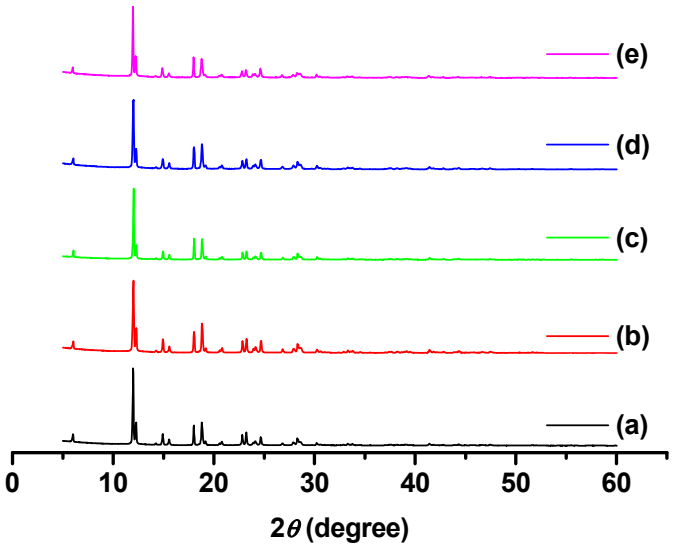

Fig. S6 PXRD patterns for **3** obtained by a series of zinc salts with different anions respectively: (a) SO_4^{2-}; (b) NO_3^-; (c) ClO_4^-; (d) Cl^-; (e) Ac^-.

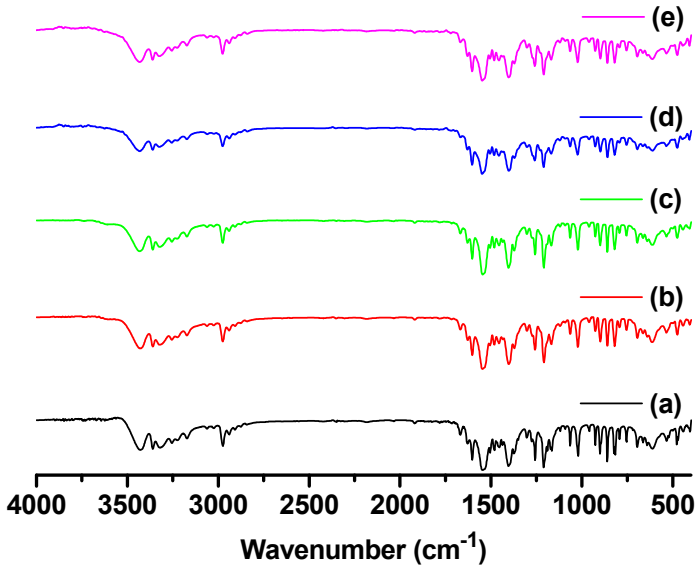

Fig. S7 IR spectra for **4** prepared by a series of cadmium salts with different anions respectively: (a) SO_4^{2-}; (b) NO_3^-; (c) ClO_4^-; (d) Cl^-; (e) Ac^-.

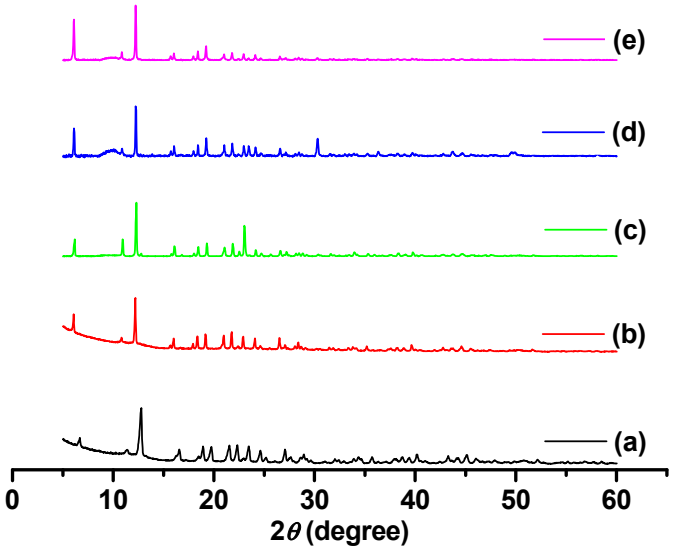

Fig. S8 PXRD patterns for **4** obtained by a series of cadmium salts with different anions respectively: (a) SO_4^{2-}; (b) NO_3^-; (c) ClO_4^-; (d) Cl^-; (e) Ac^-.

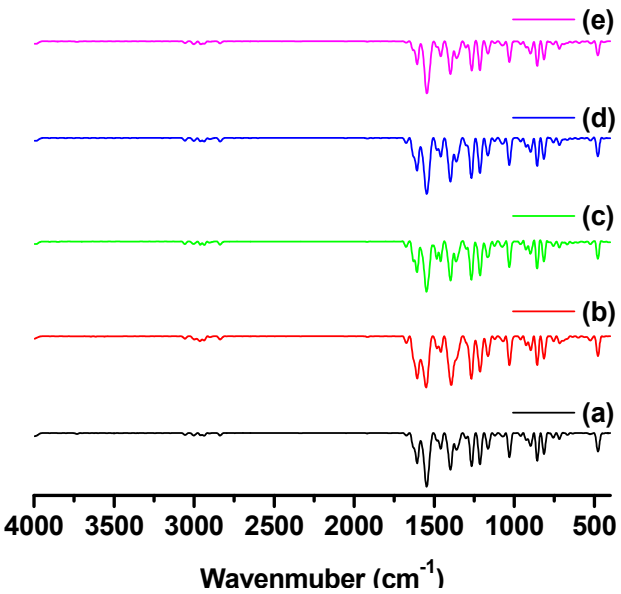

Fig. S9 IR spectra for **5** prepared by a series of cadmium salts with different anions respectively: (a) SO_4^{2-}; (b) NO_3^-; (c) ClO_4^-; (d) Cl^-; (e) Ac^-.

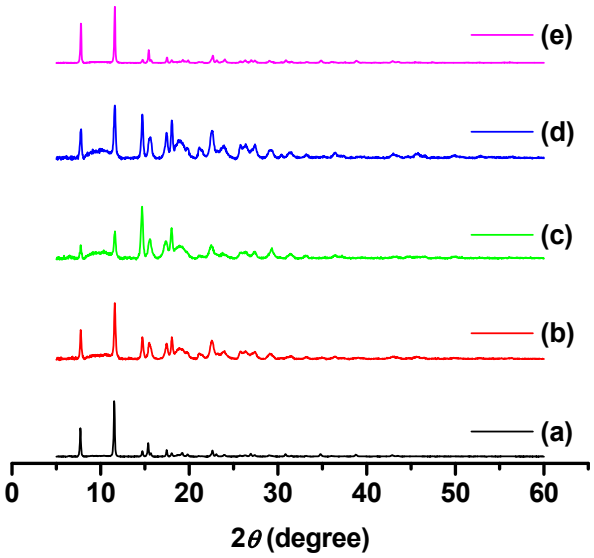

Fig. S10 PXRD patterns for **5** obtained by a series of cadmium salts with different anions respectively: (a) SO_4^{2-}; (b) NO_3^-; (c) ClO_4^-; (d) Cl^- ; (e) Ac^-.

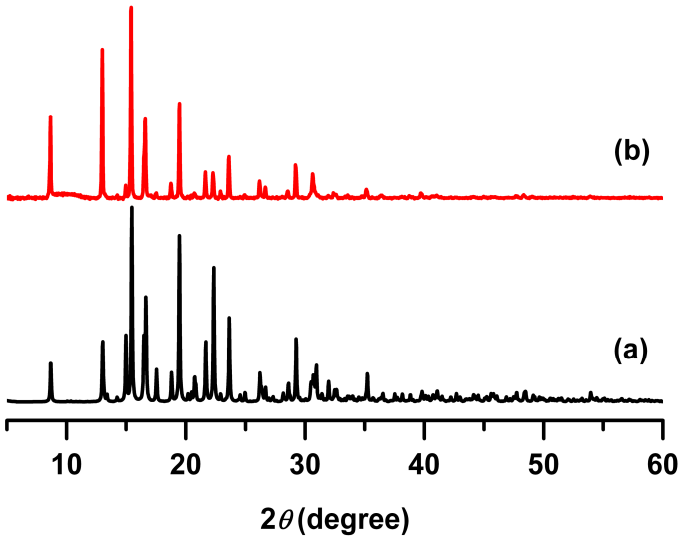

Fig. S11. X-Ray diffraction (XRD) patterns for **1**: (a) simulated; (b) powdered.

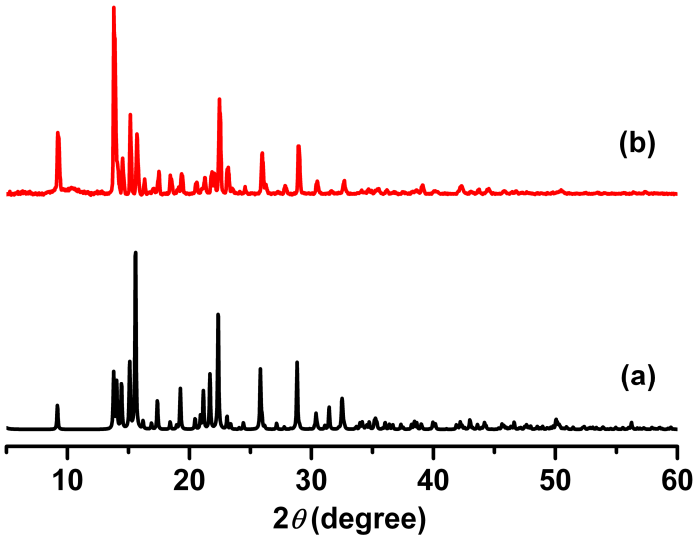

Fig. S12. XRD patterns for **2**: (a) simulated; (b) powdered.

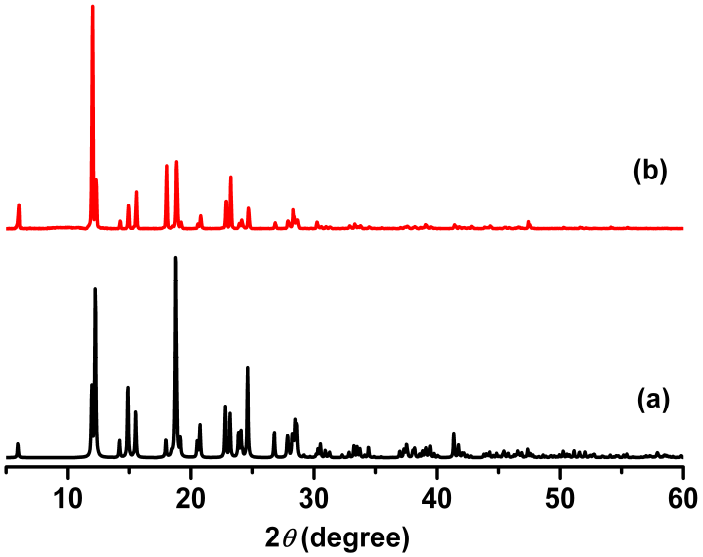

Fig. S13. XRD patterns for **3**: (a) simulated; (b) powdered.

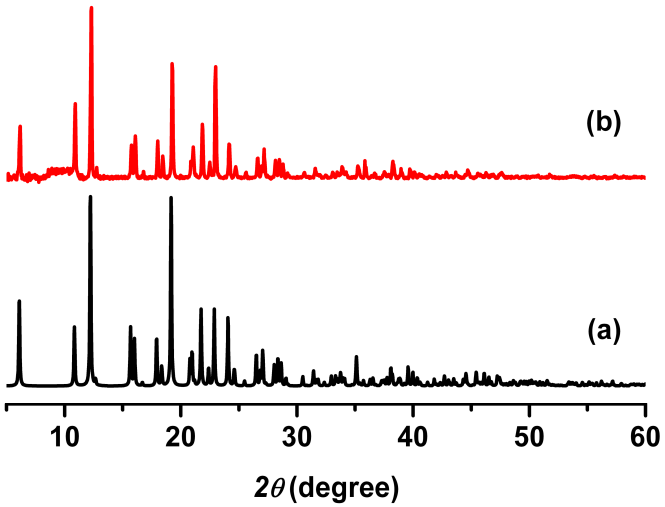

Fig. S14. XRD patterns for **4**: (a) simulated; (b) powdered.

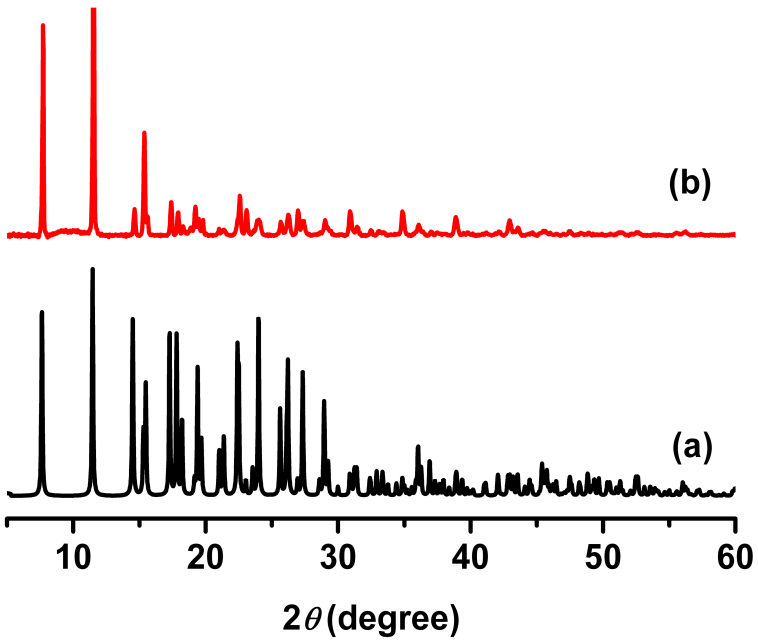

Fig. S15. XRD patterns for **5**: (a) simulated; (b) powdered.

Table S1 Selected bond lengths (Å) and angles (°) for compounds **1-5**

1			
Ni1–O4W	2.121(7)	Ni2–O11W	2.104(6)
Ni1–O5W	2.122(6)	Ni2–O10W	2.093(8)
Ni1–O6W	2.056(7)	Ni2–O12W	2.096(7)
Ni1–O3W	2.099(8)	Ni2–O7W	2.107(8)
Ni1–O1W	2.061(7)	Ni2–O9W	2.103(8)
Ni1–O2W	2.108(8)	Ni2–O8W	2.108(8)
O4W–Ni1–O6W	88.8(3)	O8W–Ni2–O11W	177.4(3)
O5W–Ni1–O6W	85.3(3)	O9W–Ni2–O11W	91.6(3)
O2W–Ni1–O4W	90.3(3)	O10W–Ni2–O12W	91.3(3)
O1W–Ni1–O2W	92.9(3)	O11W–Ni2–O12W	88.1(2)
O1W–Ni1–O3W	93.4(3)	O9W–Ni2–O12W	84.8(3)
O1W–Ni1–O4W	85.6(3)	O10W–Ni2–O11W	84.6(3)
O1W–Ni1–O5W	88.6(2)	O8W–Ni2–O9W	91.0(3)
O1W–Ni1–O6W	171.9(3)	O8W–Ni2–O10W	92.8(3)
O2W–Ni1–O3W	90.7(3)	O7W–Ni2–O8W	88.5(3)
O3W–Ni1–O4W	178.7(3)	O7W–Ni2–O9W	92.6(3)
O2W–Ni1–O5W	177.4(3)	O7W–Ni2–O10W	91.3(3)
O2W–Ni1–O6W	93.0(3)	O7W–Ni2–O11W	91.5(3)
O4W–Ni1–O5W	87.7(2)	O7W–Ni2–O12W	177.3(3)
O3W–Ni1–O5W	91.3(3)	O8W–Ni2–O12W	92.2(3)
O3W–Ni1–O6W	92.0(3)	O9W–Ni2–O10W	174.7(3)
2[i]			
Cu1–O1	1.960(2)	Cu1–O2W	1.986(4)
Cu1–O1W	2.375(5)		
O1–Cu1–O1W	85.49(17)	O1W–Cu1–O2W[a]	82.4(3)
O1–Cu1–O2W	91.72(13)	O1[a]–Cu1–O2W	88.41(13)
O1–Cu1–O1[a]	179.07(17)	O1W[a]–Cu1–O2W	82.4(3)
O1–Cu1–O1W[a]	93.61(17)	O2W–Cu1–O2W[a]	164.7(3)
O1–Cu1–O2W[a]	88.41(13)	O1[a]–Cu1–O1W[a]	85.49(17)
O1W–Cu1–O2W	112.9(3)	O1[a]–Cu1–O2W[a]	91.72(13)
O1[a]–Cu1–O1W	93.61(17)	O1W[a]–Cu1–O2W[a]	112.9(3)
O1W–Cu1–O1W[a]	31.41(17)		
3[ii]			
Zn1–O1	1.993(3)	Zn1–O1W	2.025(3)
O1–Zn1–O1W	113.89(12)	O1–Zn1–O1W[a]	112.50(12)
O1–Zn1–O1[a]	97.16(12)	O1W–Zn1–O1W[a]	106.93(14)
4[iii]			
Cd1-O1	2.384(4)	Cd1-O2	2.417(4)
Cd1-O1W	2.275(5)		

O1-Cd1-O1W	134.10(16)	O1W-Cd1-O1W^{a}	103.18(19)
O1-Cd1-O2	54.07(18)	O1W-Cd1-O2^{a}	98.91(18)
O1-Cd1-O1^{a}	78.15(14)	O2-Cd1-O2^{a}	170.8(2)
O1-Cd1-O1W^{a}	105.58(16)	O1W^{a}-Cd1-O2^{a}	86.81(18)
O1-Cd1-O2^{a}	117.57(18)		
5^{iv}			
Cd1–O1	2.433(3)	Cd1–O4	2.329(4)
Cd1–O1W	2.222(3)	Cd1–O5	2.341(3)
Cd1–O2	2.278(3)	Cd1–O1^{a}	2.254(3)
O1–Cd1–O1W	94.38(10)	O1^{a}–Cd1–O1W	92.14(11)
O1–Cd1–O2	54.97(11)	O2–Cd1–O4	150.00(12)
O1–Cd1–O4	105.85(12)	O2–Cd1–O5	100.95(11)
O1–Cd1–O5	98.19(9)	O1^{a}–Cd1–O2	93.08(11)
O1–Cd1–O1^{a}	147.78(10)	O4–Cd1–O5	55.66(11)
O1W–Cd1–O2	107.95(13)	O1^{a}–Cd1–O4	104.88(12)
O1W–Cd1–O4	95.43(12)	O1^{a}–Cd1–O5	91.23(9)
O1W–Cd1–O5	150.67(11)		

^{i}Symmetry code for **2**: ^{a} 1 - x, y, 1 - z. ^{ii}Symmetry code for **3**: ^{a} 1 - x, y, 2 - z. ^{iii}Symmetry code for **4**: ^{a} 1 - x, y, -z; ^{iv}Symmetry code for **5**: ^{a} x, -1 - y, -1/2 + z.

Table S2 Hydrogen bond geometries in the crystal structures of **1-5**

Complex	D–H···A	H···A (Å)	D···A (Å)	D–H···A (°)
1[i]	O3W–H6···O10[a]	2.48	3.300(11)	162
	O4W–H7···O8[b]	1.95	2.718(9)	150
	O13W–H26···O11[b]	2.14	2.847(11)	140
	O1W–H1···O7[b]	1.90	2.738(9)	168
	C39–H39A···O3[c]	2.56	3.430(13)	150
	O16W–H32···O7[d]	2.57	3.287(10)	143
	O16W–H32···O8[d]	2.14	2.891(9)	147
	O5W–H9···O1	1.94	2.719(9)	151
	O6W–H11···O2	1.91	2.730(9)	161
	O7W–H13···O13W	2.40	3.231(11)	165
	O7W–H14···O4	2.23	3.029(10)	157
	O8W–H16···O10	2.18	3.026(11)	172
	O12W–H23···O11	2.04	2.772(9)	144
	O12W–H24···O16W	2.00	2.770(10)	151
	O14W–H28···O7	1.83	2.674(9)	172
	O15W–H30···O1	2.21	2.890(10)	137
2[ii]	O1W–H1WA···O2[a]	2.19	2.716(6)	120
	O1W–H1WB···O3W[a]	1.88	2.360(10)	114
	O3W–H3WB···O1W[b]	1.70	2.360(10)	132
	O3W–H3WB···O2	2.41	3.017(12)	129
3[iii]	O2W–H2WA···O1W[a]	2.27	3.016(7)	147
	O2W–H2WB···O1[b]	1.98	2.817(7)	167
	C11W–H11A···O2[c]	2.60	3.448(6)	148
4[iv]	O1W–H1WA···O2W	2.54	3.317(5)	152
	O1W–H1WB···O1[a]	2.24	3.058(7)	162
	O2W–H2WA···O2[b]	1.98	2.756(6)	151
	C11–H11A···O2W[c]	2.59	3.423(7)	143
	C14–H14A···O1[d]	2.53	3.397(7)	151
5[v]	O1W–H1WB···O5[a]	1.94	2.753(4)	159
	C2–H2···O2[a]	2.51	3.335(5)	142
	O1W–H1WA···O5[b]	1.99	2.768(4)	152

[i]Symmetry codes for **1**: [a] –1 + x, 1 + y, z; [b]–1 + x, y, z; [c] 1 + x, -1 + y, -1 + z; [d] x, -1 + y, z. [ii]Symmetry codes for **2**: [a] x, -1 + y, z; [b] x, 1 + y, z. [iii]Symmetry codes for **3**: [a] x, 1 + y, z; [b] 1-x, y, 2 - z; [c] 3/2 - x, 1/2 + y, 2 - z. [iv]Symmetry codes for **4**: [a] 1-x, -1 + y, - z; [b] 1 - x, y, 1 - z; [c] x, 1 + y, z; [d] 3/2 - x, 1/2 + y, - z.
[v]Symmetry codes for **5**: [a] x, -1- y, 1/2 + z; [b] x, -1 + y, z.

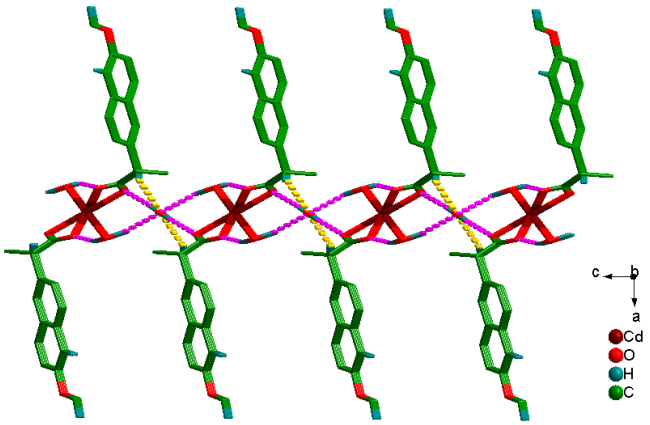

Fig. S16. A 2D layer along the *b* axis in **4**.

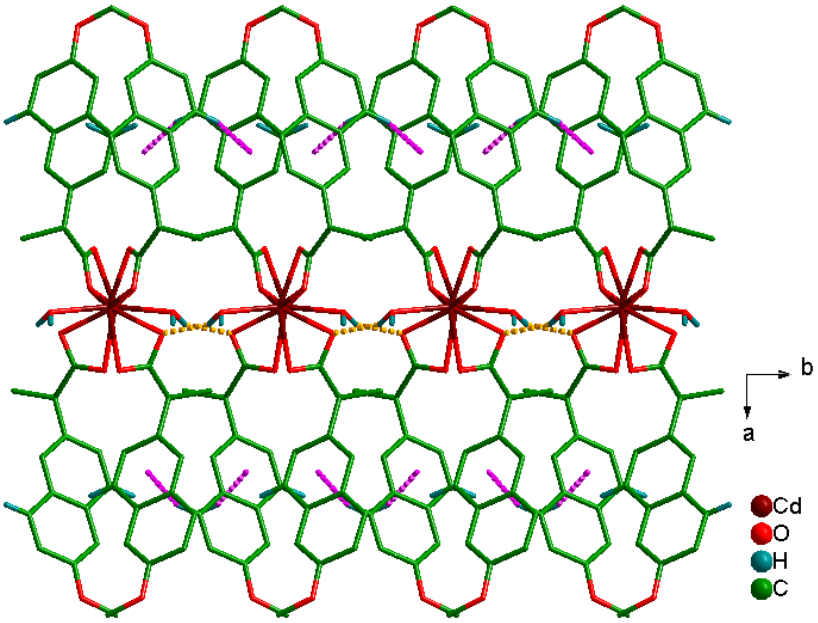

Fig. S17. A 2D layer along the *c* axis in **5**.

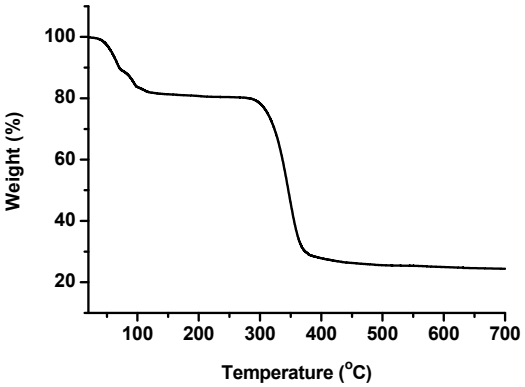

(a)

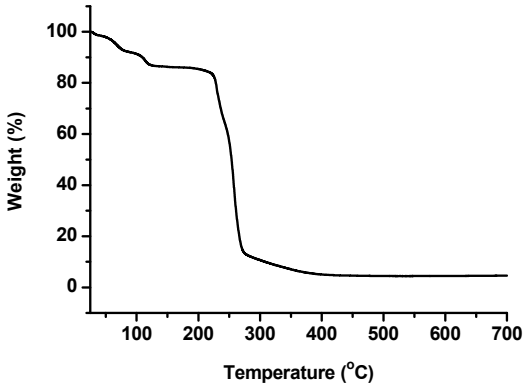

(b)

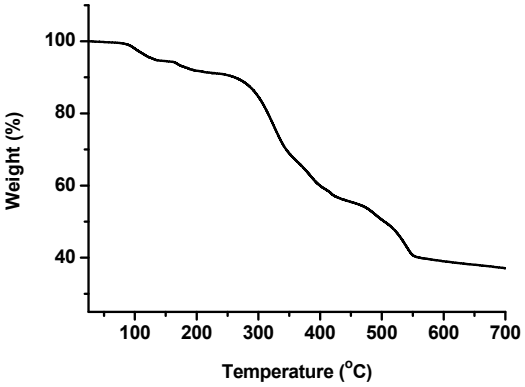

(c)

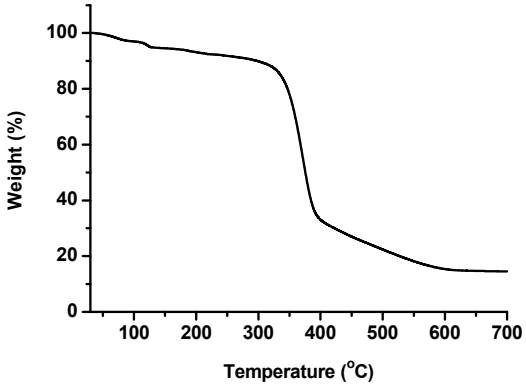

(d)

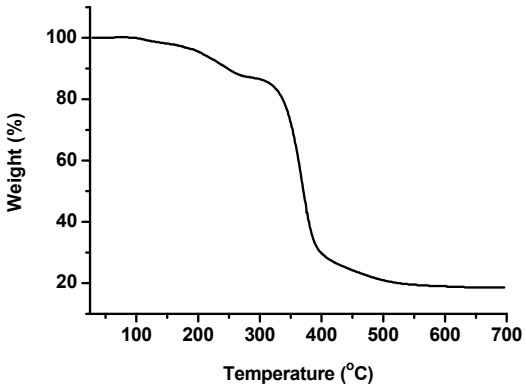

(e)

Fig. S18. TGA cures of complexes **1**-**5**; (a) for **1**; (b) for **2**; (c) for **3**; (d) for **4**; (e) for **5**.

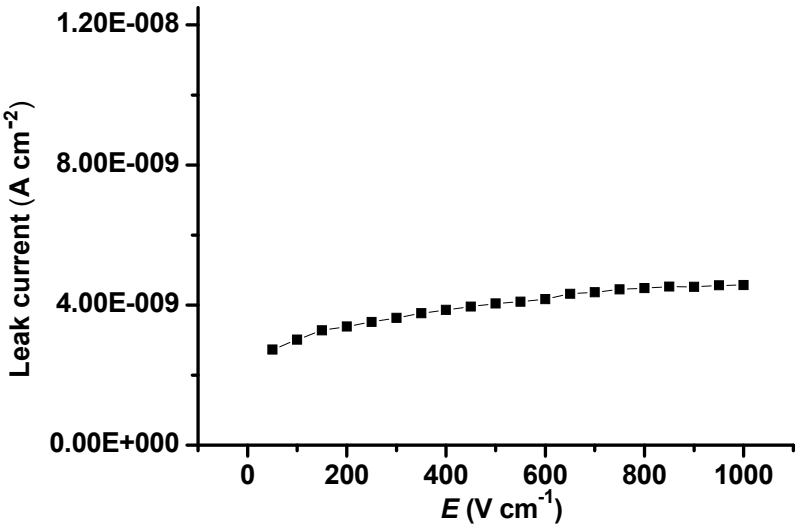

(a)

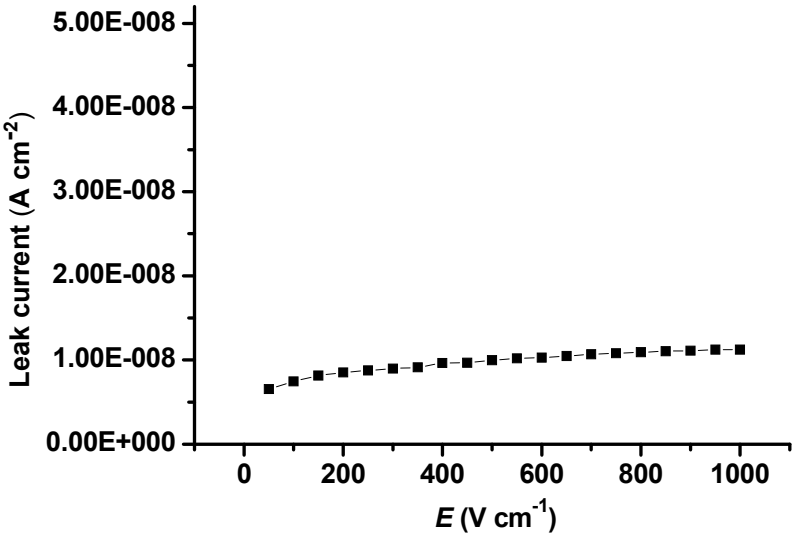

(b)

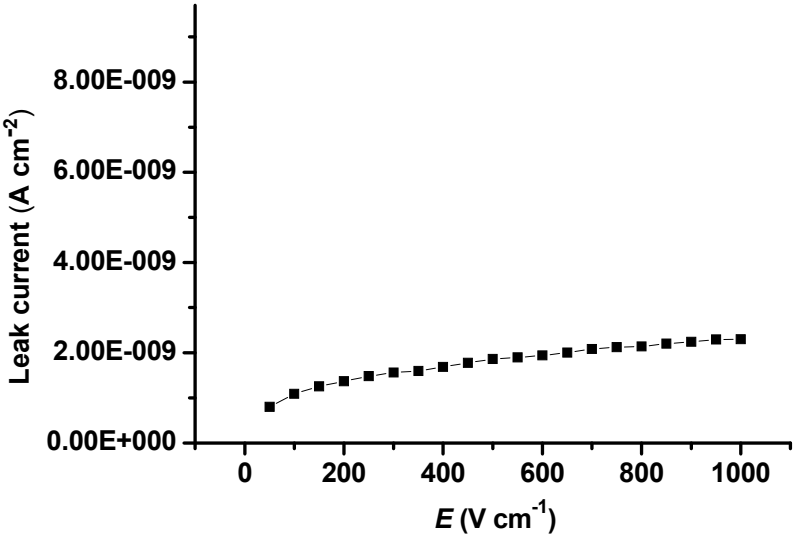

(c)

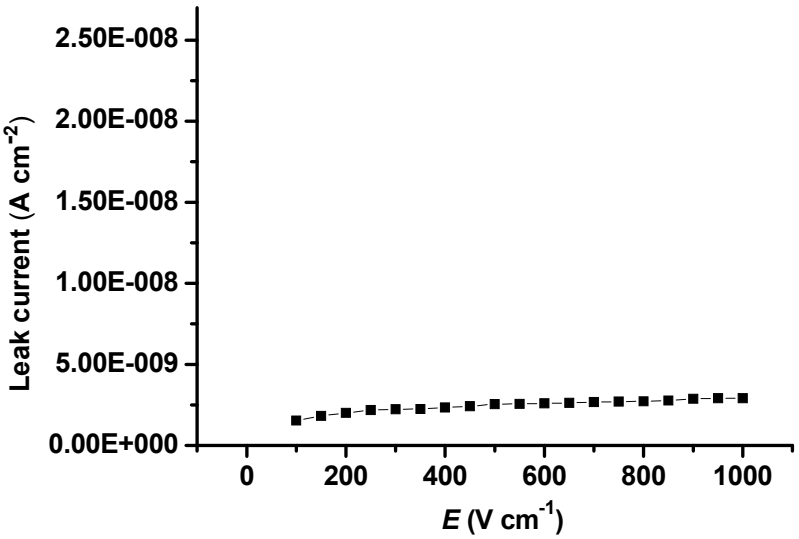

(d)

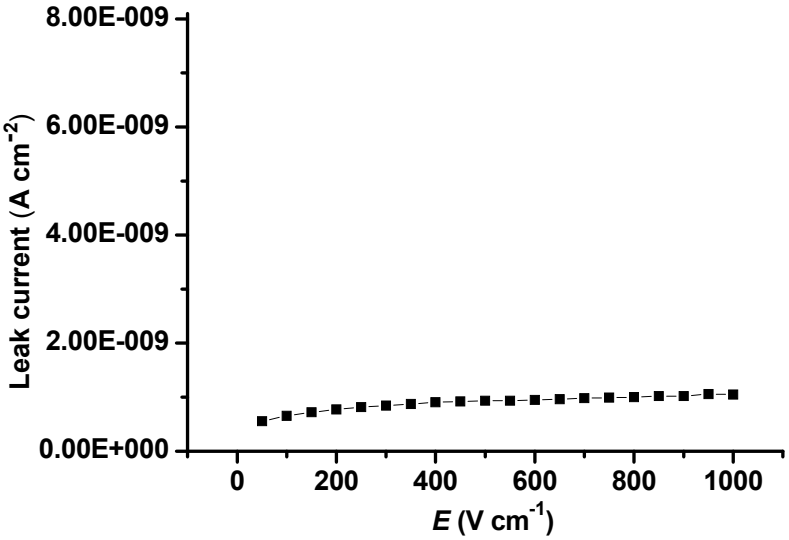

(e)

Fig. S19 Plots of leakage current in compounds **1** (a), **2**(b), **3**(c), **4**(d), and **5**(e), respectively.